EPJ Web of Conferences will be set by the publisher
DOI: will be set by the publisher
© Owned by the authors, published by EDP Sciences, 2016

arXiv:1601.05025v1 [hep-ex] 19 Jan 2016

Highlights from the COMPASS experiment at CERN

Hadron spectroscopy and excitations

Frank Nerling[1,a], on behalf of the COMPASS Collaboration

[1] *Universität Mainz, Institut für Kernphysik, Germany*

Abstract. The COMPASS experiment at the CERN-SPS studies the spectrum and the structure of hadrons by scattering high energy hadrons and polarised muons off various fixed targets. Recent results for the hadron programme comprise highlights from different topics. A selective overview is given and, among others, the following results are discussed. The precise determination of the pion polarisability, a long standing puzzle that has been solved now, is presented as well as measurements of radiative widths. The observation of a new narrow axial-vector state, the $a_1(1420)$, as well as deeper insights into the exotic 1^{-+}-wave, which is under study since decades by several experiments, are discussed and further, the search for the charmonium-like exotic $Z_c(3900)$ state in the COMPASS data is covered.

1 Introduction

The COMPASS fixed-target experiment [1] at CERN-SPS is a facility to study quantum chromodynamics (QCD). It is dedicated to study the perturbative and non-perturbative regime of QCD, and probe the structure and dynamics of hadrons. Using a muon beam, COMPASS investigates nucleon structure by measuring helicity, transversity and general parton distribution functions — the recent highlights from the COMPASS muon programme are summarised in [2]. Hadron excitations and spectroscopy, including the search for exotic states, are investigated using hadron beams on a liquid hydrogen (proton) and different nuclear targets. A selection of recent results of the COMPASS hadron programme are discussed and summarised here.

The two-stage spectrometer (Fig. 1) is equipped with electromagnetic and hadronic calorimeters, providing detection of charged and neutral final state particles with a homogeneous acceptance over a wide kinematic range, especially covering a large range in momentum transfer. At lowest reduced four-momentum transfers between the beam particle and the target of $t' < 10^{-3}\,(\mathrm{GeV}/c)^2$, Primakoff reactions are studied, from which the pion polarisability has been extracted at high experimental precision, Chiral perturbation theory (ChPT) is tested and the radiative decay widths of the $a_2(1320)$ and the $\pi_2(1670)$ have been measured in pion-photon reactions. At low four-momentum transfers of $0.1\,(\mathrm{GeV}/c)^2 < t' < 1\,(\mathrm{GeV}/c)^2$, the mass spectrum of hadrons is investigated, including searches for (spin-) exotic mesons.

[a] e-mail: nerling@cern.ch

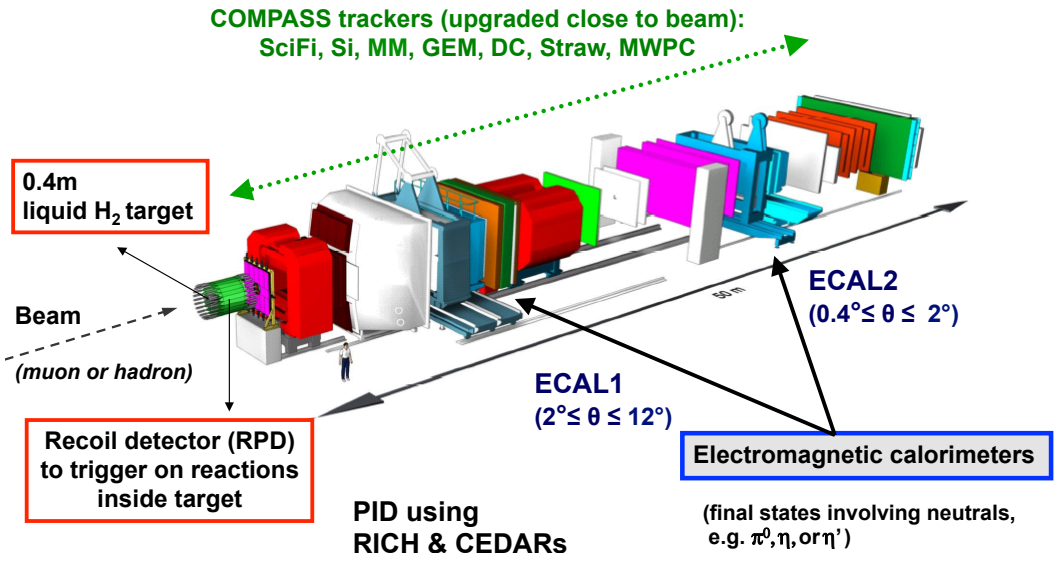

Figure 1. Schematic drawing of the COMPASS two-stage spectrometer as used for the hadron runs 2008/09.

2 Results on hadron excitations

For the understanding of QCD and the low-momentum expansion ChPT, in which the pions are identified as the Goldstone bosons as a result of the spontaneous chiral symmetry breaking, the pion properties are a crucial input. Whereas pion-pion scattering has extensively been studied and successfully described within ChPT, experimental results of pion-photon reactions in terms of the most basic process provided still a puzzle: Previous measurements of the pion polarisability, the leading structure-dependent term of Compton scattering, provided resultant values significantly larger as expected from theory, *cf.* Fig. 2. Apart from the pion polarisability in Primakoff reactions (Sec. 2.1), also pion-photon interactions with more than one pion in the final state are studied (Secs. 2.2 and 2.3).

2.1 Measurement of pion polarisability

The rigidity of an extended object against deformations by an external electric or magnetic field are described by the so-called electric and magnetic polarisabilities α and β, respectively. As the pion is not a point-like particle, it is sensitive to deformations by such external fields, and this tiny effect, called pion polarisability, is under the assumption of $\alpha_\pi = -\beta_\pi$ predicted in Chiral Perturbation Theory (ChPT) to be 5.7×10^{-4} fm^3 [3].

Polarisabilities are usually measured in Compton scattering experiments. Even though pions can hardly be used as a fixed-target, they can be scattered off the Coulomb potential of a heavy nucleus, like a Nickel (Ni) target. In the corresponding $\pi^-\gamma \to \pi^-\gamma$ scattering process, the polarisabilities manifest as a deviation from the Born cross-section of a point-like particle. The measurement of the cross-section of this process allows to extract the pion polarisabilities via the deviation from the assumption for a point-like particle.

Such a measurement is experimentally demanding and the systematics need precisely to be controlled. An important advantage of the COMPASS experiment is that we can perform this measurement with the pion and with the muon beam (quickly switchable within about two hours), in which the latter acts as a control measurement of the point-like muon.

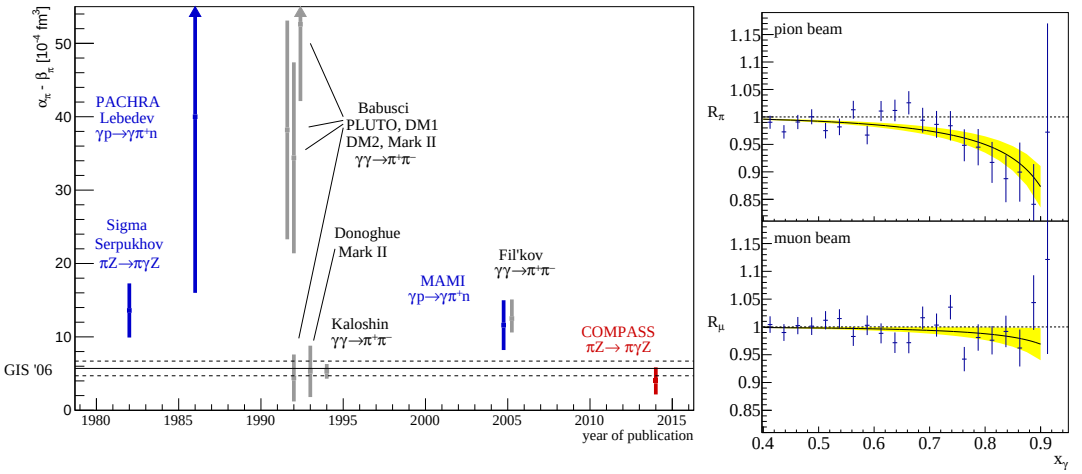

Figure 2. *Left*: Compilation of experimental measurements of the pion polarisability $\alpha_\pi - \beta_\pi$ including the new COMPASS result and the theoretical prediction from ChPT [3], plot taken from [4]. *Right:* Ratio R of the measured cross-section over the simulated one for a point-like object for the pion beam data *(top)* and for the control measurement with the muon beam data *(bottom)* [5].

The COMPASS data of scattering a pion beam off a Ni target comprises the Compton part of the cross-section [5]. The $\pi^- Ni \to \pi^- \gamma Ni$ events are selected by requiring one negatively charged track from the vertex inside the Ni target, a high-energetic shower in the electromagnetic calorimeters for the final state photon, whereas the photon exchange is ensured by a cut on low photon virtualities Q^2, energy conservation is applied to select exclusive reactions, *i.e.* $\Delta E = E_{beam} - E_{\pi'} - E_\gamma \approx 0$, neglecting the (tiny) nuclear recoil energy. In order to stay in the kinematic region of stable trigger and muon identification efficiencies, the ratio of the final state photon and the initial beam energy $x_\gamma = E_\gamma / E_{beam}$ is required to be between 0.4 and 0.9. Under the assumption of $\alpha_\pi = -\beta_\pi$ that has to be made due to the limited statistics at lower x_γ (*i.e.* the phase space region sensitive to $\alpha_\pi + \beta_\pi$), the polarisation should manifest in terms of a decreasing ratio R of the measured cross-section over the simulated one for a point-like particle with increasing x_γ. This behaviour has exactly been measured for the pion beam data, *i.e.* for the extended object of the pion, as displayed in Fig. 2 (right, top). To extract the polarisability α_π from the measured ratio R, the photon energy spectrum is examined according to the following relation, which is a simplified relation of the Primakoff cross-section in one-photon exchange approximation:

$$R = \frac{\sigma(x_\gamma)}{\sigma_{\alpha_\pi=0}(x_\gamma)} = 1 - \frac{3}{2} \cdot \frac{{m_\pi}^3}{\alpha} \cdot \frac{{x_\gamma}^2}{1 - x_\gamma} \alpha_\pi .$$

For the muon beam data (Fig. 2, right, bottom), the size of the fake polarisability of $(0.5 \pm 0.5_{stat}) \times 10^{-4}$ fm^3 is within the statistical uncertainty compatible with zero. This value is taken as an estimate of the systematic error due to apparative imperfections, not described by the MC simulation. For the pion beam data (Fig. 2, right, top), a pion polarisability of $\alpha_\pi = (2.0 \pm 0.6_{stat}) \times 10^{-4}$ fm^3 is determined from the fit. This pion polarisability value measured by COMPASS is in tension with previous experiments and in agreement with the prediction from ChPT (Fig. 2, left).

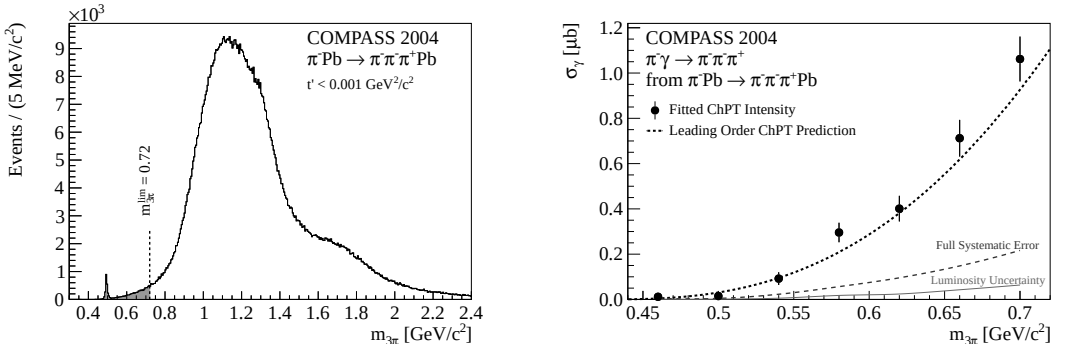

Figure 3. *Left:* Spectrum of the 3π mass from $\pi^- Pb \to \pi^-\pi^+\pi^- Pb$ in the Primakoff region of four-momentum transfer $t' < 10^{-3}\,\mathrm{GeV}^2/c^2$. The region of interest in view of ChPT up to $m_{3\pi} \approx 0.72\,\mathrm{GeV}/c^2$ is indicated. At $m_{K^-} \approx 0.49\,\mathrm{GeV}/c^2$, a peak from the admixture of incident beam kaons decaying into $(3\pi)^-$ is visible that are used for flux normalisation. *Right:* First measurement of the photo-production cross-section σ_γ in this mass range, found in agreement with the prediction from leading order ChPT [6].

2.2 Measurement of chiral dynamics

From the same data, further processes on chiral dynamics are accessible, like *e.g.* the chiral anomaly in $\pi^-\gamma \to \pi^-\gamma$, the corresponding analysis is still under way, the same holds for the neutral pion case of two-pion production $\pi^-\gamma \to \pi^-\pi^0\pi^0$ at low energy. Based on the 2004 pilot run data (Primakoff kinematics), the two-pion production for the charged case $\pi^-\gamma \to \pi^-\pi^+\pi^-$ has been analysed [6].

Figure 3 (left) shows the mass spectrum of the outgoing three-pion final state. Of particular interest in view of chiral dynamics is the low mass tail up to three pion masses, as indicated in the figure. Performing a partial-wave analysis (PWA) including amplitudes from ChPT calculations substituting the isobaric partial waves in this mass range, after flux normalisation on the observed kaon decays (using the kaon admixture in the beam), the absolute cross-section is, within the experimental uncertainty of 20 %, found in agreement with the leading order ChPT prediction.

In the 3π mass spectrum (Fig. 3, left), structures from the well-known resonances $a_1(1260)$ and $a_2(1320)$ are visible at higher masses — the corresponding radiative couplings have been measured as discussed in the next section (Sec. 2.3).

2.3 Measurement of radiative width

Electromagnetic transitions can be measured via radiative decays of a resonance $X \to \pi\gamma$. The direct measurement of $\pi\gamma$ is experimentally difficult. Alternatively, the inverse process of scattering a pion off a Coulomb field producing an intermediate resonance X, *i.e.* the Primakoff reaction, can be used. The Coulomb potential of a heavy nucleus acts as a (quasi-real) photon source, and the Primakoff production cross-section of a resonance X is proportional to the width of the radiative decay of that resonance: $\sigma_{\text{Primakoff}}(X) \sim \Gamma_0(X \to \pi\gamma)$. Due to the exchange particle being a quasi-real photon, Primakoff produced resonances have predominantly spin projection M=1. Even though states with spin projection M=1 can also be produced diffractively, the cross-section here is proportional to $t'^{|M|}e^{-bt'}$, so that the diffractive production is highly suppressed at very small values of t'.

Based on the negative pion beam data on a thin lead (Pb) target, the COMPASS Collaboration studied this reaction and measured the radiative widths of the $a_2(1320)$ and the $\pi_2(1670)$ [7]. Performing a partial-wave analysis, the data is decomposed into spin-parity states, and thus also the M=1 states are identified. To extract the radiative widths of the $a_2(1320)$ and the $\pi_2(1670)$,

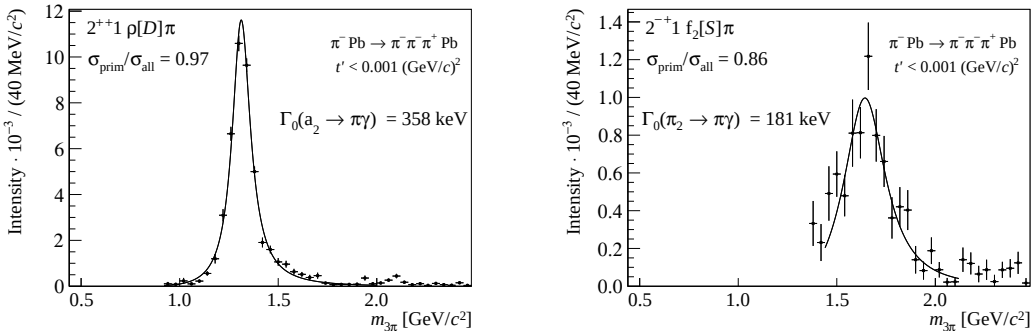
$2^{++}1\ \rho[D]\pi$
$\sigma_{prim}/\sigma_{all} = 0.97$
$\pi^- Pb \to \pi^-\pi^-\pi^+ Pb$
$t' < 0.001\ (GeV/c)^2$
$\Gamma_0(a_2 \to \pi\gamma) = 358$ keV
Intensity $\cdot 10^{-3}$ / (40 MeV/c^2)
$m_{3\pi}$ [GeV/c^2]
$2^{-+}1\ f_2[S]\pi$
$\sigma_{prim}/\sigma_{all} = 0.86$
$\pi^- Pb \to \pi^-\pi^-\pi^+ Pb$
$t' < 0.001\ (GeV/c)^2$
$\Gamma_0(\pi_2 \to \pi\gamma) = 181$ keV
Intensity $\cdot 10^{-3}$ / (40 MeV/c^2)
$m_{3\pi}$ [GeV/c^2]

Figure 4. Results of the measured radiative widths of the $a_2(1320)$ *(left)* and the $\pi_2(1670)$ *(right)* (reprinted with kind permission of EPJ from [7], copyright Società Italiana di Fisica / Springer-Verlag 2014). As compared to previous measurements, the COMPASS result for the $a_2(1320)$ is the most precise one, whereas for the $\pi_2(1670)$, the COMPASS value is the first measurement at all.

the two partial waves $J^{PC}M^{\epsilon}\,(isobar)\,\pi = 2^{++}1^{\epsilon}\rho(770)\pi$ D-wave and $2^{-+}1^{\epsilon}f_2(1270)\pi$ S-wave have been considered, respectively. For the events analysed, namely at $t'<10^{-3}\,\mathrm{GeV}^2/\mathrm{c}^2$, the contribution of Primakoff production is 97 % and 86 % of the intensities found in the $2^{++}1^{\epsilon}\rho(770)\pi\,D$ and $2^{-+}1^{\epsilon}f_2(1270)\pi$ S-waves, respectively. The intensities for the two different reflectivities $\epsilon = \pm 1$ have to be summed up incoherently as the production plane at such small t' is not measured sufficiently precise due to limited experimental resolution. That there are further possible decay channels (than $\rho(770)\pi$ for the $a_2(1320)$ and $f_2(1270)\pi$ for the $\pi_2(1670)$) has been taken into account by consideration of the relevant branching fractions. The fits to the data are shown in Fig. 4, from which a width of $\Gamma_0(a_2(1320) \to \pi\gamma) = (358\pm6\pm42)$ keV and $\Gamma_0(\pi_2(1670) \to \pi\gamma) = (181\pm11\pm27)$ keV have been measured for the $a_2(1320)$ and the $\pi_2(1670)$, respectively. Both results are consistent with predictions based on the VMD model [8]. Compared to previous measurements, the COMPASS result for $\Gamma_0(a_2(1320) \to \pi\gamma)$ is the most precise one, whereas for $\Gamma_0(\pi_2(1670) \to \pi\gamma)$ the COMPASS result is the first measurement at all.

3 Results on hadron spectroscopy

There are many states that have been observed so far in the light meson sector, whereas quite some of the observations still need confirmation. Comparing the experimental situation to the predictions based on the naive quark model, quite some agreement is found, however, not all the predictions are perfectly consistent with experiment: Some of the predicted states have not yet been observed, also there are observed states that are not expected, see *e.g.* [9]. Given the relatively large widths of many of these states ($\sim$100 MeV/c^2) together with the high level density of the mesons with (u,d,s) constituent quarks, there are quite some overlaps and mixing, complicating the analyses.

Of particular interest are exotic mesons, not fitting the constituent quark model. QCD allows for and predicts such states, like glue-balls, hybrids or tetraquarks according to various models. Mesons of same spin-parity quantum numbers mix, and the unambiguous observation is thus difficult. So-called spin-exotic states with J^{PC} quantum numbers not accessible by a simple $q\bar{q}$ configuration are on the other hand very promising to search for as they do not mix with ordinary mesons. The experimental observation of such spin-exotic states would be a fundamental confirmation of QCD, for a recent overview, see *e.g.* [10].

The COMPASS data give access to all decay channels spin-exotic hybrid candidates have been reported in so far by different experiments, like $\rho(770)\pi$, $\eta(')\pi$, $f_1(1285)\pi$ and $b_1(1235)\pi$. The lightest

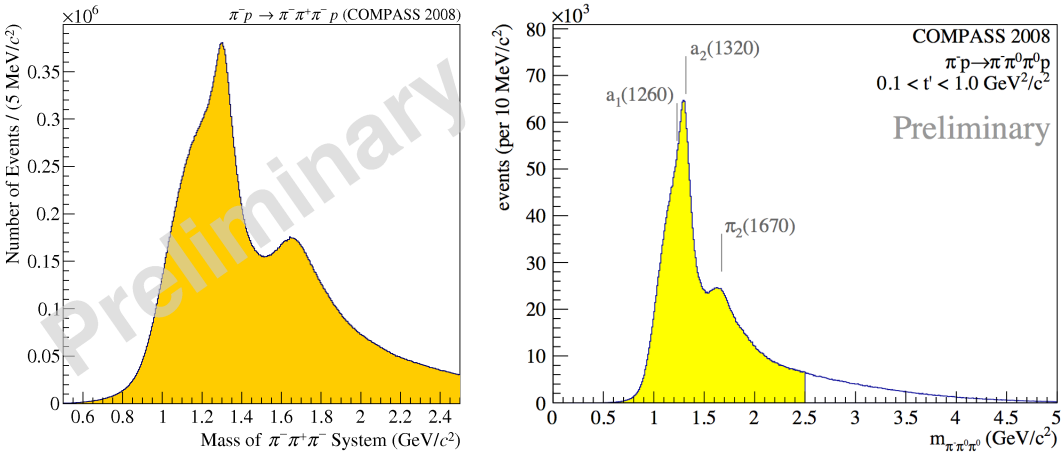

Figure 5. Invariant mass spectrum of the exclusively produced, outgoing $(3\pi)^-$ system for the charged *(left)* and the neutral *(right)* decay modes [14, 15].

hybrid candidate with exotic $J^{PC} = 1^{-+}$, the famous $\pi_1(1600)$, has been searched for and is studied in two different decay channels simultaneously, namely in $\pi^-\pi^+\pi^-$ and $\pi^-\pi^0\pi^0$ final states [11–16] produced in diffractive pion dissociation $\pi^- p \to (3\pi)^- p'$. Since the reconstruction depends on different parts of the detector, the observation of a state in both channels provides an independent confirmation within the same experiment, the possibility of cross-checks and control of systematics.

The invariant mass of the diffractively produced $(3\pi)^-$ system is shown for the charged and neutral $\rho\pi$ decay modes in Fig. 5 (left) and (right), respectively. In the range of four-momentum transfer $0.1\,(\mathrm{GeV}/c)^2 < t' < 1.0\,(\mathrm{GeV}/c)^2$ used for PWA, about 50 million and 3.5 million exclusive $(3\pi)^-$ events have been reconstructed from the 2008 data (of negative pion beam impinging on a proton target) in the mass range of 0.5 and 2.5 GeV/c^2 for the charged and the neutral mode, respectively. By the interaction with the target, the beam pion is excited to an intermediate resonance X^- that subsequently decays into a di-pion resonance, the so-called isobar decaying into two pions, and a bachelor pion with the relative orbital angular momentum L between them. For the results presented here, the $\rho(770)$, $f_0(980)$, $f_2(1270)$, $f_0(1500)$, $\rho_3(1690)$ and a broad $(\pi\pi)_s$ component have been used. The set of partial waves contains 87 partial waves up to $L = 6$ and an incoherent wave, the so-called "flat wave", having an isotropic angular distribution, representing events of three uncorrelated pions.

Given the observed dependence on t' and the large statistics, the PWA method has been extended with respect to the scheme of a two-step PWA as applied previously, for a complete description including all details, see [17]. The data has been divided into 11 and 8 bins of t' such that about equal statistics is contained in each bin, and (as previously) into 20 MeV/c^2 and 40 MeV/c^2 wide $m_{3\pi}$ bins for the charged and the neutral mode data, respectively. The first step analysis, the so-called mass-independent PWA, is carried out independently for each mass bin and independently for the different ranges of t'. This maximum likelihood (rank-1) fit of the model to the data extracts the production amplitudes, taking into account the detector acceptance. Finally, the analysis is completed by the second step analysis, the so-called mass-dependent fit. In this χ^2 fit of Breit-Wigner amplitudes to a subset of the spin density matrix, resonance parameters are extracted, for which not only the intensities but also the interferences are taken into account. Also it takes into account the observed t' dependencies by performing a simultaneous optimisation of the resonant parameters in all t' regions.

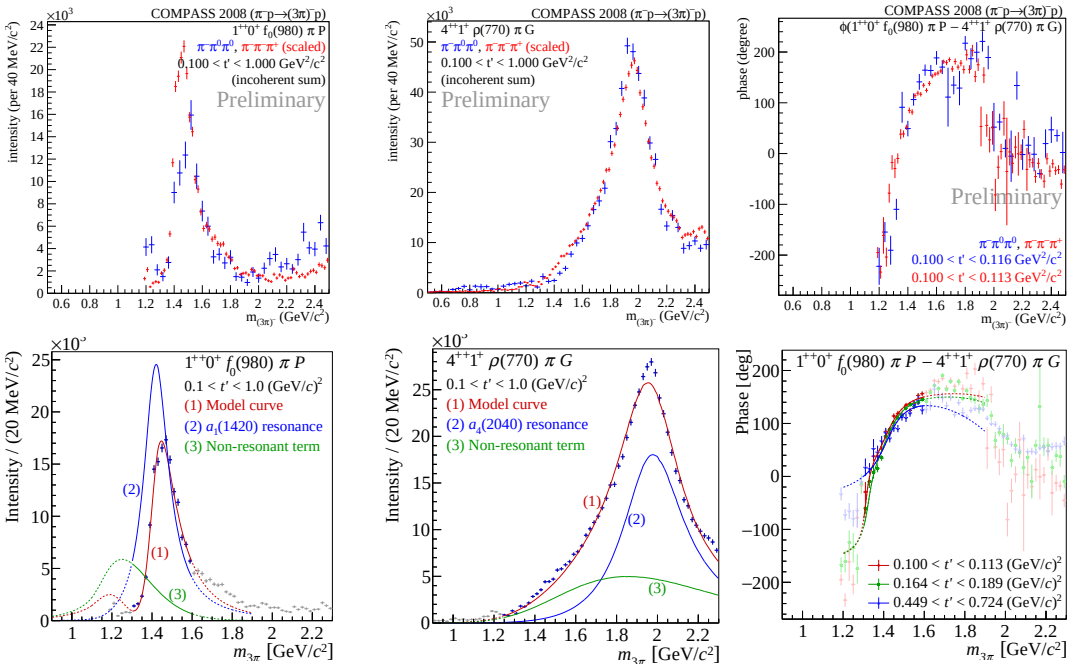
COMPASS 2008 (π⁻p→(3π)⁻p)
1⁺⁺0⁺ f₀(980) π P
π⁻π⁰π⁰, π⁻π⁻π⁺ (scaled)
0.100 < t' < 1.000 GeV²/c²
(incoherent sum)
Preliminary
intensity (per 40 MeV/c²)
m(3π)⁻ (GeV/c²)
4⁺⁺1⁺ ρ(770) π G
phase (degree)
ϕ(1⁺⁺0⁺ f₀(980) π P − 4⁺⁺1⁺ ρ(770) π G)
0.100 < t' < 0.116 GeV²/c²
0.100 < t' < 0.113 GeV²/c²
0.1 < t' < 1.0 (GeV/c)²
(1) Model curve
(2) a₁(1420) resonance
(3) Non-resonant term
Intensity / (20 MeV/c²)
m3π [GeV/c²]
(2) a₄(2040) resonance
Phase [deg]
0.100 < t' < 0.113 (GeV/c)²
0.164 < t' < 0.189 (GeV/c)²
0.449 < t' < 0.724 (GeV/c)²

Figure 6. *Top:* First step PWA result, charged versus neutral decay mode [14]: The fitted intensity for the $1^{++}0^{+}$ $f_0(980)\,\pi$ P-wave shows a narrow structure at about 1.4 GeV/c^2, it is similarly observed for both, neutral and charged $(3\pi)^-$ mode *(left)*. In the resultant intensity for the $4^{++}1^{+}$ $\rho(770)\,\pi$ G-wave, the known $a_4(2040)$ is similarly observed *(centre)*. The relative phase of the two shows a clean rapid phase motion in the signal region. *Bottom:* Second step PWA result, charged decay mode [18]: Complete fit result in terms of the resultant $1^{++}0^{+}$ $f_0(980)\,\pi\,P$ intensity (incoherent sum over t' ranges) *(left)*, the first step result is given by the black data points and the resonance model fit overlaid in red consists of the BW describing the narrow structure, that we call the $a_1(1420)$ (blue curve), and the non-resonant background contribution (green curve). The corresponding result is shown for the $a_4(2040)$ observed in the $4^{++}1^{+}$ $\rho(770)\,\pi$ G-wave *(centre)*. The relative phase of the $a_1(1420)$ against the $a_4(2040)$ *(right)* is shown for three different t' ranges, consistently showing a clean rapid phase rotation in the signal region.

3.1 Observation of a new axial-vector state $a_1(1420)$

Figure 6 (top/left) shows the first step PWA result for one out of the 87 partial waves, namely the $1^{++}0^{+}$ $f_0(980)\pi$ P-wave, in terms of the fitted intensity for both decay modes. Indeed, the incoherent sum over the different t' ranges is shown here, and the charged is normalised to the neutral mode data using the integral. Good agreement on the fit result is found for the two channels. For both decay modes, the $1^{++}0^{+}$ $f_0(980)\pi$ P-wave intensity, containing only a very small fraction of the total observed intensity of about 0.25 % [18], shows a clear signal slightly above 1.4 GeV/c^2. Rapid phase rotations with respect to known resonances, like *e.g.* the $a_4(2040)$ (Fig. 6, top/centre), are observed in the signal region (Fig. 6, top/right), as it is expected for a resonance. A phase does not depend on the amount of amplitude, and the phase motion is observed independent of t'.

In the second analysis step, a Breit-Wigner resonance model with a minimal set of three waves is used, namely the $2^{++}1^{+}$ $\rho(770)\pi$ D, $4^{++}1^{+}$ $\rho(770)\pi$ G and $1^{++}0^{+}$ $f_0(980)\pi$ P waves. For the charged mode data, the completed PWA result is show for the $1^{++}0^{+}$ $f_0(980)\pi$ P-wave in Fig. 6 (bottom/left) and for the $4^{++}0^{+}$ $\rho(770)\pi$ G-wave in Fig. 6 (bottom/centre), the phase difference between them is given in Fig. 6 (bottom/right). From this fit, we obtain a mass of $m = 1414^{+15}_{-13}$ MeV/c^2 and a width

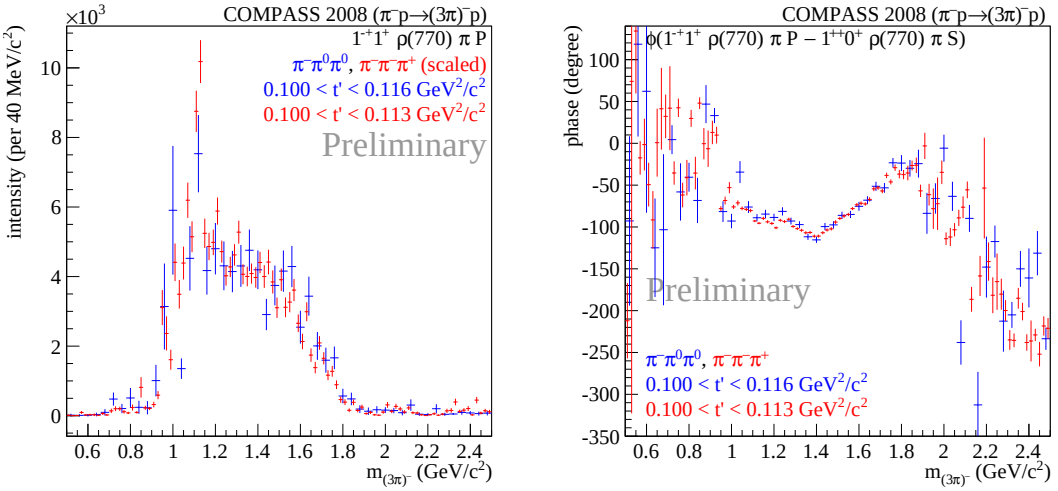

Figure 7. First step PWA result for the exotic $1^{-+}1^{+}\,\rho(770)\pi$ P-wave in $(3\pi)^{-}$ final states, charged versus neutral mode data. The resultant fitted intensities are found in good agreement for the two channels *(left)*. Shown are the results for the lowest range of four-momentum transfer t', where the signal on top of the broad bump at about 1.6 GeVc^2 has the lowest evidence as compared to the higher t' regions, in which the signal to background ratio improves with increasing t'. The relative phases with respect to the $1^{++}0^{+}\,\rho(770)\pi$ S-wave, in which the well-known $a_1(1260)$ resonance is observed, is displayed *(right)*, showing a clean phase motion in the range of about 1.4 and 1.8 GeV/c^2 consistently for the two decay modes.

of $\Gamma = 153^{+8}_{-23}$ MeV/c^2. The interpretation of this new isovector state is still unclear. The properties of the $a_1(1420)$ suggest it to be the isospin partner of the $f_1(1420)$, especially supported by the strong coupling to the $f_0(980)$ (and not to ρ) that is interpretable as a $K\bar{K}$ molecule. The $a_1(1420)$ and the $f_1(1420)$ may possibly be the first observed isospin partners for a $K\bar{K}\pi$ moleculartype excitation, which suggests further studies of the $K\bar{K}\pi$ final state. A first, very promising look at the $f_1(1420)$ observed decaying to $K\bar{K}\pi$ in the (same) COMPASS 2008 data set has already been provided [19], including first very preliminary PWA confirming (due to spin assignment) the state in the $K\bar{K}\pi$ invariant mass indeed to be the $f_1(1420)$ and not the $\eta(1295)$.

3.2 Status of the search for the spin-exotic $\pi_1(1600)$ resonance

In the 2004 pilot run data (π^- beam, Pb target), a significant J^{PC} spin-exotic signal has been observed at $1660\pm10^{+0}_{-64}$ MeV/c^2. It shows a clean phase motion against well-known resonances and is consistent with the disputed $\pi_1(1600)$ [20]. The high statistics of the 2008 proton target data allows the search for exotic states in different decay modes in the same experiment [11]. Employing the same PWA method as in [20], the results obtained for the $(1^{-+})1^{+}\rho^{-}\pi^{0}$ and $(1^{-+})1^{+}\rho^{0}\pi^{-}$ intensity and relative phase are similar and consistent with the previous observations [12, 13]. Apart of the established resonances $a_1(1260)$, $a_2(1320)$, $\pi_2(1670)$, also $\pi(1800)$ and $a_4(2040)$, an exotic signal in the 1^{-+} wave at around 1.6 GeV/c^2 has been observed, that shows a clean phase motion with respect to well-known resonances. These results are consistently obtained for both $\rho\pi$ decay modes, neutral and charged. The extension to an additional t' binning and performing the PWA independently also in different ranges of t' [17] allows for disentangling resonant from non-resonant particle production (*e.g.* dynamically produced components caused by the Deck effect [21]).

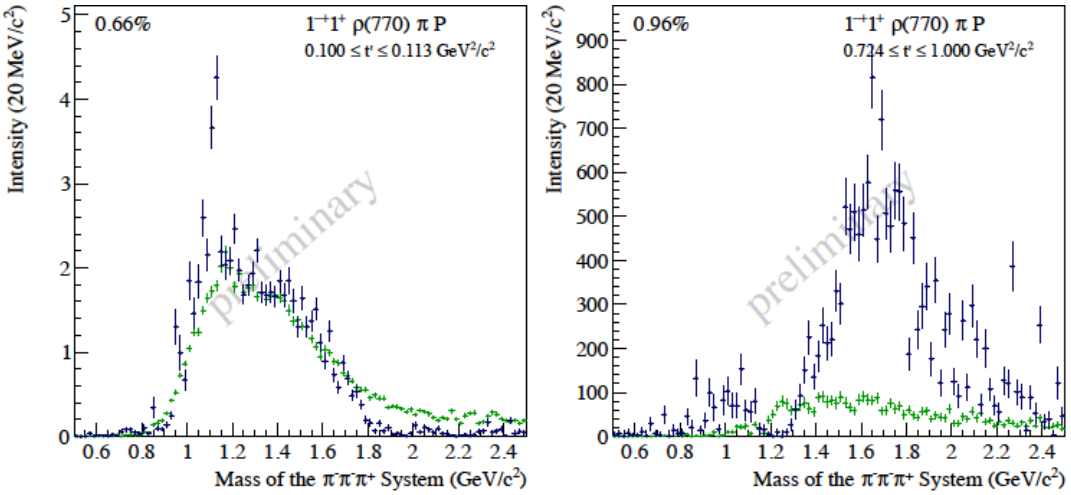

Figure 8. First step PWA result for the intensity of the exotic $1^{-+}1^{+}\,\rho(770)\,\pi$ P-wave for the charged decay mode (blue) overlaid with a projection of a simulated Deck-effect in this wave (green), shown for the range of lowest *(left)* and highest *(right)* values of t' [16].

A dependency of the exotic $1^{-+}1^{+}\,\rho(770)\pi\,P$ wave intensity on the squared four-momentum t' is observed. Whereas a significant signal is observed at around $1.6\,\mathrm{GeV}/c^2$ on top of a moderate background at larger values of t', the signal to background ratio decreases with decreasing t'. The fitted intensity of the exotic $1^{-+}1^{+}\,\rho(770)\pi\,P$ wave is shown for the range of smallest t' for the charged and neutral decay modes in Fig. 7 (left). Apart from the good agreement between the two channels, we observe mainly a broad bump. Even though there is hardly evidence for a signal at about $1.6\,\mathrm{GeV}/c^2$ in this plot, *i.e.* for this t' range of $0.100 < t' < 0.113\,\mathrm{GeV}/c^2$, the corresponding relative phase with respect to the $1^{++}0^{+}\,\rho(770)\pi$ S-wave, in which the well-known $a_1(1260)$ is observed, a clean phase motion is consistently observed for the two different decay modes in the range of about 1.4 and $1.8\,\mathrm{GeV}/c^2$. This is exactly the mass range where a significant exotic 1^{-+} signal is observed for ranges of larger t' (see e.g. Fig. 8, right). The relative phase of two resonances is independent of the given absolute amplitudes, and a consistent phase motion is observed in all bins of t'.

The observed dependency of the signal to background ratio on t' could be caused by the interference of a resonance with a large non-resonant background contribution, possibly introduced and to be explained by the Deck effect [21]. In order to further investigate this explanation, pseudo data were generated according to a dedicated model [22]. This data has been analysed as the real data, including the decomposition into partial waves, in order to study the Deck-amplitude contribution to the different partial waves included in the PWA. Figure 8 shows the promising outcome of the study for the exotic 1^{-+} partial wave, exemplary for the ranges of smallest and largest t' for the charged decay mode. The Deck amplitude intensities are normalised to the total intensity (summed over all mass and t' bins) in the given wave. A large part of the exotic 1^{-+} wave intensity at small values of t' can be described as a contribution by the non-resonant Deck process (Fig. 8, left), whereas the contribution at large t' is almost negligible according to this ansatz.

For completeness, further relevant results and ongoing analyses that are not dicussed in detail here are the PWA results of diffractive $(\eta\pi)^-$ and $(\eta'\pi)^-$ production [23] and preliminary PWA results for central production (*i.e.* via double pomeron exchange) of $\pi^+\pi^-$ and K^+K^- from the 2009 COMPASS proton beam data [24].

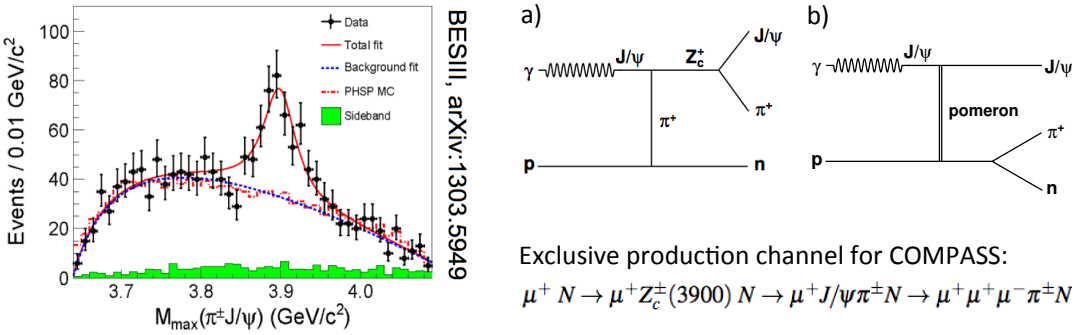

Figure 9. *Left:* The charmonium-like exotic state $Z_c(3900)$ decaying to $J/\psi\pi^{\pm}$ as observed by BESIII [26]. *Right:* In the COMPASS muon data, the $Z_c(3900)$ should be produced via photoproduction according to the process given under a), the main background originates from pomeron exchange reactions, b).

3.3 Search for the manifestly exotic $Z_c(3900)$ state

Even though the COMPASS muon beam data is mainly dedicated to study (spin-dependent) parton distribution functions, a hadron spectroscopy result has been obtained based on the full set of COMPASS data collected with a muon beam between 2002 and 2011, namely an upper limit on the photoproduction of the $Z_c(3900)$ [25]. The charged charmonium-like exotic state $Z_c(3900)$ was observed decaying to $J/\psi\pi^{\pm}$ by the BESIII [26] Collaboration and confirmed by Belle [27] in 2013, see Fig. 9 (left) for the observation plot, later also the neutral partner was confirmed [28].

As the photon may act as a J/ψ according to the VDM, the $Z_c(3900)$ should be produced via interaction of the incoming photon with the virtual pion from the nucleon target according to the diagram in Fig. 9 (right, a), and the cross-section for this process should be sizable [29].

The reconstructed exclusive production channel is $\mu^+N \rightarrow \mu^+Z_c^{\pm}(3900)N \rightarrow \mu^+J/\psi\pi^{\pm}N$, with J/ψ decaying to $\mu^+\mu^-$, means the final state to detect is $\mu^+\mu^+\mu^-\pi^{\pm}N$. The event selection of the exclusively produced $\mu^+J/\psi\pi^{\pm}$ is straight forward: A vertex is reconstrcuted having exactly three outgoing muons and a pion, to identify the J/ψ, a mass cut on the reconstructed $\mu^+\mu^-$ invariant mass is applied as indicated in Fig. 10 (left), energy balance is requested and, in order to suppress background from pomeron exchange reactions (Fig. 10, right, b), a momentum cut $p_{\pi^{\pm}} > 2\,\mathrm{GeV/c}$ for the pions is applied. In addition, in order to make use of the measurement of the cross-section $\sigma(\gamma N \rightarrow J/\psi N)$ provided by the NA14 experiment [30] for absolute normalisation, the exclusive μ^+J/ψ sample is selected as well using the same selection criteria. The ratio of acceptances for both samples equals in first approximation about the acceptance for the additional pion that we know to be $0.5 \pm 0.1_{syst}$, averaged over all setup and target configuartions.

The resultant COMPASS plot for the search for the $Z_c(3900)$ is given in Fig.10 (right), where the reconstructed $J/\psi\pi$ invariant mass is plotted and the expectation region for a signal of the $Z_c(3900)$ is indicated. No signal of exclusive photoproduction of the $Z_c^{\pm}(3900)$ state and the decay into $J/\psi\,\pi^{\pm}$ has been found. Thus, an upper limit was determined on the product of the cross-section and the relative $Z_c^{\pm}(3900) \rightarrow J/\psi\pi^{\pm}$ decay probability normalised to the cross-section of incoherent exclusive

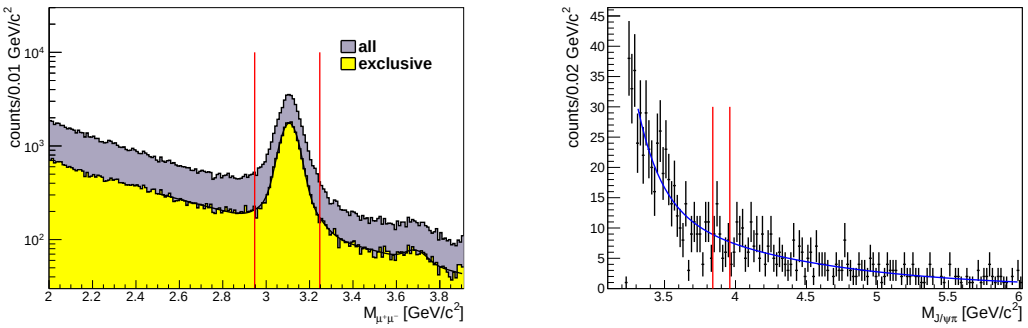

Figure 10. *Left:* Reconstructed $\mu^+\mu^-$ invariant mass for all events and for the exclusive sample selected, the mass cut applied to identify the J/ψ is indicated. *Right:* Final plot of the reconstructed $J/\psi\pi$ invariant mass distribution, where the mass range of the expected $Z_c(3900)$ signal is indicated — no signal is observed [25].

photo-production of J/ψ mesons. We obtain the following result [25]

$$\frac{BR(Z_c^{\pm}(3900) \to J/\psi\,\pi^{\pm}) \times \sigma_{\gamma\,N \to Z_c^{\pm}(3900)\,N}}{\sigma_{\gamma\,N \to J/\psi\,N}}\Big|_{\langle\sqrt{s_{\gamma N}}\rangle = 13.8\ GeV} < 3.7 \times 10^{-3}\,. \tag{1}$$

Assuming $\sigma_{\gamma\,N \to J/\psi\,N} = 14.0 \pm 1.6_{\text{stat.}} \pm 2.5_{\text{syst.}}$ nb as measured by the NA14 Collaboration for $\sqrt{s}_{\gamma\,N} = 13.7\ GeV$ [30], the result can be presented as

$$BR(Z_c^{\pm}(3900) \to J/\psi\,\pi^{\pm}) \times \sigma_{\gamma\,N \to Z_c^{\pm}(3900)\,N}\Big|_{\langle\sqrt{s_{\gamma\,N}}\rangle = 13.8\ GeV} < 52\ \text{pb}. \tag{2}$$

This result has been obtained within the framework of the Z_c production mechanism proposed in Ref. [29]. Unless the assumptions made therein are wrong, a conclusion is that the regarded decay channel $Z_c^{\pm}(3900) \to J/\psi\,\pi^{\pm}$ can not be the dominant one. This result is an important input for the clarification of the nature of this charmonium-like $Z_c^{\pm}(3900)$ state that due to the charge and the quark content of $c\bar{c}$ is manifestly an exotic one.

3.4 Summary and outlook

The COMPASS experiment at CERN/SPS is well suited for high precision measurements in the fields of hadron excitations and spectroscopy, completing together with the hadron structure studies the broad and rich COMPASS hadron physics programme.

Chiral perturbation theory has been confirmed by the COMPASS measurement of the pion polarisability $(\alpha_\pi - \beta_\pi)$ at high precision, and chiral dynamics has been observed (again in agreement with ChPT) in the process $\pi\gamma \to 3\pi$ at low relative momenta. Moreover, radiative couplings of meson resonances have been measured at unprecedented precision.

A possible new isovector resonance with $J^{PC} = 1^{++}$, a mass of about 1420 MeV/c^2 and a width of about 150 MeV c^2 has been observed in $f_0(980)\pi P$ decay mode. It shows a rapid phase motion with respect to established resonances. The extension to a t'-resolved partial-wave analysis provides deeper understanding of the exotic signal that we observe at around 1.6 GeV/c^2 in the $1^{-+}1^+\,\rho(770)\pi\,P$ wave, showing resonant behaviour. The intensity observed at small momentum transfers t' seems to a large extent to be attributed to contributions from the Deck effect, whereas merely a negligible Deck contribution seems to play a role at larger values of t'. Deeper insights on the disputed $\pi_1(1600)$ hybrid candidate are not only gained via the two $(3\pi)^-$ decay channels but also in the $\eta\pi$ and $\eta'\pi$ channels.

As an outlook, the 2012 Primakoff data set with considerably larger statistics will further improve the pion polarisability measurement. Thanks to the extended x_γ range, also a measurement of $(\alpha_\pi+\beta_\pi)$ will be feasible, also a first measurement of the kaon polarisability is foreseen. For spectroscopy, the analysis of $(5\pi)^-$, $(\eta\eta\pi)^-$ and also $(f_1\pi)^-$ will allow for access towards higher masses, and complete the list of channels for spin-exotic search.

References

[1] COMPASS Collaboration, P. Abbon *et al.*, Nucl. Instrum. Meth. **A577** (2007) 455-518, Nucl. Instrum. Meth. **A779** (2015) 69-115; arXiv:1410.1797 [phys./ins-det].

[2] S. Platchkov, for the collaboration, these proceedings (2015).

[3] J. Gasser, M.A. Ivanov, and M.E. Sainio, Nucl. Phys. B **745**, 84 (2006).

[4] T. Nagel, PhD thesis, TU München (2012), CERN-THESIS-2012-138.

[5] COMPASS Collaboration, C. Adolph *et al.*, Phys. Rev. Lett. **114**, 062002 (2015).

[6] COMPASS Collaboration, C. Adolph *et al.*, Phys. Rev. Lett. **108**, 192001 (2012).

[7] COMPASS Collaboration, C. Adolph *et al.*, European Physical Journal A **50**, 79 (2014).

[8] J.L. Rosner, Phys. Rev. D **23**, 1127 (1981).

[9] J. Beringer *et al.*, (Particle Data Group), Phys. Rev. D **86** (2012) 010001.

[10] C.A. Meyer, Y. Van Haarlem, Phys. Rev. C **82**, 025208 (2010).

[11] F. Nerling, for the collaboration, AIP Conf. Proc. **1257** (2010) 286; arXiv:1007.2951[hep-ex].

[12] F. Haas, for the collaboration, Conf. Proc., Hadron2011, Munich (2011); arXiv:1109.1789v2[hep-ex].

[13] F. Nerling, for the collaboration, Conf. Proc. MESON2012, EPJ Web Conf. 37, 09025 (2012); arXive:1401.4943[hep-ex].

[14] S. Uhl, for the collaboration, Conf. Proc. Hadron2013, PoS, 087 (2013); arXive:1401.4943v2[hep-ex].

[15] F. Haas, PhD thesis, TU München, January 2014; CERN-THESIS-2013-277.

[16] S. Uhl, for the collaboration, Conf. Proc. PANIC 2014, DESY-PROC-2014-04, 169 (2014).

[17] COMPASS Collaboration, C. Adolph *et al.*, subm. to Phys. Rev. D, (2015); arXiv:1509.00992[hep-ex].

[18] COMPASS Collaboration, C. Adolph *et al.*, Phys. Rev. Lett. **115**, 082001 (2015).

[19] J. Bernhard and F. Nerling, for the collaboration, Conf. Proc. Hadron2011, Munich (2011); arXiv:1109.0219[hep-ex].

[20] COMPASS collaboration, M. Alekseev *et al.*, Phys. Rev. Lett, **104**, 241803 (2010).

[21] R.T. Deck, Phys. Rev. Lett. **13**, 169 (1964).

[22] C. Daum *et al.*, Nucl. Phys. B **182**, 269 (1981).

[23] COMPASS Collaboration, C. Adolph *et al.*, Phys. Lett. B **740**, 303 (2015).

[24] A. Austregesilo, Conf. Proc. Hadron2013, PoS, 102 (2013).

[25] COMPASS Collaboration, C. Adolph *et al.*, Phys. Lett. **B742**, 330 (2015).

[26] BESIII Collaboration, M. Ablikim *et al.*, Phys. Rev. Lett. **110**, 252001 (2013).

[27] Belle Collaboration, Z.Q. Liu *et al.*, Phys. Rev. Lett. **111**, 019901 (2013).

[28] BESIII Collaboration, M. Ablikim *et al.*, Phys. Rev. Lett. **113**, 212002 (2014).

[29] Q.-Y. Lin *et al.*, Phys. Rev. D **88**, 114009 (2013); arXiv:1304.0121[hep-ex].

[30] NA14 Collaboration, R. Barate *et al.*, Z. Phys. C **33**, 505, (1987).